Absence of long-range order in a three-dimensional geometrically frustrated antiferromagnet

J. N. Reimers*
Institute for Materials Research, McMaster University, Hamilton, Ontario, Canada L8S 4M1
(Received 15 May 1991; revised manuscript received 26 August 1991)

Classical Heisenberg spins on a lattice of *corner*-sharing tetrahedra with nearest-neighbor antiferromagnetic interactions are investigated with Monte Carlo (MC) techniques. The system is highly frustrated with an infinitely degenerate ground state. Mean-field theory predicts no long-range order (LRO) at any temperature. The MC calculations are consistent with this result, thus providing evidence that thermal fluctuations beyond the mean-field approximation do not stabilize LRO. The possibility of incommensurate and spin nematic order is considered. The temperature dependence of some spin-glass order parameters, such as the Edwards-Anderson order parameter and the single-spin autocorrelation function, are also investigated. The results show that no spin freezing occurs at nonzero temperatures.

I. INTRODUCTION

Frustration in magnetic systems is well known to be responsible for a number of diverse phenomena such as spin-glass behavior,[1] noncollinear and incommensurate order,[2] unusual critical properties,[3] and infinitely degenerate ground states. The stacked triangular lattice antiferromagnet[4] and the fcc antiferromagnet[5] with Ising spins are examples of three-dimensional systems with infinitely degenerate ground states. However, these systems have the interesting property that long-range order (LRO) is stabilized at finite temperatures. Frustrated systems with XY or Heisenberg spins will tend to find noncollinear long-range-ordered states at low temperatures. The best known example is the 120° spin structure found in triangular lattice antiferromagnets.

Pyrochlores have the chemical composition $A_2B_2O_7$ and crystallize in the cubic, face-centered space group $Fd\bar{3}m$, where the A and B atoms are metals located on the sites 16c and 16d of the space group. Each of the metal atoms in this system forms an infinite three-dimensional lattice of *corner*- sharing tetrahedra. If either of the A or B atoms is magnetic, then there is a very high degree of frustration when the nearest-neighbor interactions are antiferromagnetic. A schematic diagram of the tetrahedra formed by the 16c lattice within a unit cell is shown in Fig. 1, the 16d sublattice is identical except for a spatial displacement of $(\frac{1}{2},\frac{1}{2},\frac{1}{2})$. Frustration on a lattice of *corner*- sharing tetrahedra can be partially understood by realizing that no spin configuration exists which simultaneously satisfies all six antiferromagnetic interactions on a single tetrahedron. This same difficulty is also present on the fcc lattice which can be thought of as a lattice of *edge*- sharing tetrahedra. LRO in pyrochlores is further inhibited because the tetrahedra are corner-sharing and thus more sparsely connected than in the fcc counterpart.

The problem of antiferromagnetic ordering on this lattice has been considered by Anderson,[6] who predicted on qualitative grounds a very high ground-state degeneracy and that no LRO would exist at any temperature for Ising spins. Villain reached basically the same conclusion for Heisenberg spins,[7] calling the system a "cooperative paramagnet." Monte Carlo (MC) simulations with Ising spins[8] are consistent with this result. More recently, mean-field calculations have shown that Fourier spin modes with arbitrary wave vector are degenerate.[9] This implies that no LRO occurs within the mean-field approximation. Another interesting problem is that of quantum spins on the corner-sharing tetrahedral lattice with antiferromagnetic interactions. Initial work on this difficult problem is also consistent with a lack of conventional LRO.[10]

Through a simple application of counting degrees of freedom, one can show that the ground-state manifold of a pyrochlore antiferromagnet with N Heisenberg spins is at least $N/2$ dimensional. Each spin has two degrees of freedom, $\{\theta,\phi\}$, for a total of $2N$ degrees of freedom in a system with N spins. There are $N/2$ tetrahedra in the system (four spins per tetrahedron and each spin is shared by two tetrahedra). The ground-state condition

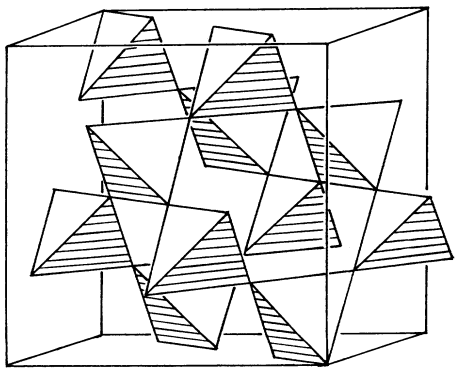

FIG. 1. The three-dimensional network of corner-sharing tetrahedra formed by one of the metal sublattices in pyrochlores. An outline of the cubic unit cell is also shown.

for a single tetrahedron is

$$\mathbf{S}_1+\mathbf{S}_2+\mathbf{S}_3+\mathbf{S}_4=\mathbf{0}\ , \tag{1}$$

which gives *at most* $\frac{3}{2}N$ constraints on the system that must be satisfied in the ground state. We say at most $\frac{3}{2}N$ because, in all likelihood, the conditions are not linearly independent. In any case, this leaves *at least* $N/2$ remaining continuous degrees of freedom in the system. Thus, the ground-state degeneracy is macroscopic and therefore not long-range ordered. However, the question remains as to whether or not thermal fluctuations beyond the mean-field level will stabilize LRO.

It is instructive to compare the pyrochlore antiferromagnet with the fcc Heisenberg antiferromagnet since the fcc lattice can be thought of as a network of edge-sharing tetrahedra. The type-I fcc antiferromagnet exhibits LRO at finite temperature and a finite ground-state degeneracy per spin.[11] However, at the mean-field level of approximation, there is a two-dimensional continuous degeneracy with respect to the relative orientations of the four magnetic sublattices. Henley has shown that thermal fluctuations will break this degeneracy and select a collinear ordered phase, i.e., two spins up and two spins down.[12] This process of thermal selection has been termed "order by disorder."[13] With this result in mind, it is interesting to consider whether or not thermal fluctuations will break the enormous degeneracy evident at the mean-field level in the pyrochlore problem.

The theoretical work is augmented by a significant amount of intriguing experimental results that point towards spin-glass-like behavior. One class of materials is the defect pyrochlores $CsMnFeF_6$ and $CsNiFeF_6$. In these compounds Cs is on the 8b sites and the two transition elements are disordered on the 16c sites.[14] Thus, there is a significant structural difference with the pyrochlore oxides which show no obvious signs of disorder. Extensive measurements have been reported which indicate some behavior similar to that of spin glasses but other effects which are contrary to such a characterization. Cusps in the low-field dc and ac susceptibility are reported along with differences in zero-field-cooled and field-cooled behavior, and remnant magnetism at low temperatures.[15–19]

The other class of pyrochlores which we call spin-glass-like are the oxides with general formula $R_2M_2O_7$, where R is a trivalent rare earth and M is a transition metal. Crystallographic information on the series of compounds $R_2Mn_2O_7$ (R = Dy–Lu,Y) (Ref. 20) obtained by single-crystal x-ray diffraction showed no evidence for disorder. Spin-glass-like behavior in $Y_2Mn_2O_7$ is evidenced by the following: (1) heat-capacity measurements show large entropy removal down to 2 K and no sharp anomaly associated with a phase transition, (2) irreversibilities in the dc susceptibility, (3) frequency dependence of the ac susceptibility maximum, and (4) diffuse neutron scattering over a wide temperature range in the absence of any magnetic Bragg peaks.[21]

The related compound $Y_2Mo_2O_7$ shows spin-glass-behavior[22] in the form of a cusp and sample history dependence in the magnetic susceptibility, even though the compound appears to be chemically ordered.[23] Similar behavior has also been observed in susceptibility data for $Tb_2Mo_2O_7$.[24] Here spin-glass-like behavior is also evident in neutron-diffraction data where strong diffuse magnetic scattering develops below the apparent freezing temperature of 25 K. In fact, inelastic-neutron-scattering measurements on $Tb_2Mo_2O_7$ show direct evidence for some degree of spin freezing near 25 K.[25]

The question of chemical order in these oxide pyrochlores requires that more careful work be carried out. Cation disorder can be ruled out on the basis of bond length arguments. The transition-metal site is quite simply too small to accommodate the rare-earth ions. However, the possibility of oxygen nonstoichiometry at the 1–5 % level is not unreasonable.

Recently there has been some interest in the stacked Kagomé lattice system $SrCr_{8-x}Ga_{4+x}O_{19}$.[26–28] This system also exhibits diffuse neutron scattering over a wide temperature range down to 1.5 K and other spin-glass properties. This is indeed interesting in light of the fact that the Kagomé lattice, which is also very highly frustrated, can be thought of as a lattice of corner-sharing triangles and is therefore a natural two-dimensional analog of the corner-sharing tetrahedral lattice. Between every other Kagomé sheet in $SrCr_{8-x}Ga_{4+x}O_{19}$ is a triangular plane of Cr^{3+} ions situated above and below the centers of the Kagomé triangles thus forming distorted tetrahedra (see Ref. 23 for a drawing). The mean-field-theory results for the Kagomé and pyrochlore systems are almost identical.[9] Recent theoretical work[29] on Kagomé lattice antiferromagnets suggests an infinitely degenerate ground state and no LRO at any temperature for Heisenberg spins in the absence of further neighbor interactions.

The aim of this work is to determine the effects of thermal fluctuations on antiferromagnetic ordering in pyrochlores. In particular, it is important to establish whether or not thermal fluctuations will significantly lift the Fourier mode degeneracy present at the mean-field level of approximation. Also, attempts will be made to determine the dynamics of some spin-glass order parameters. The paper is organized as follows: In Sec. II we describe the details of the MC methods used. Elementary thermodynamic properties for a chemically ordered pyrochlore model, with only nearest-neighbor interactions and classical vector spins, will be described in Sec. III. The powder neutron-scattering function is shown in Sec. IV and a check for spin nematic order can be found in Sec. V. Section VI focuses on the behavior of various spin-glass order parameters calculated by the MC simulations. Concluding comments can be found in Sec. VII.

II. MONTE CARLO METHOD

A standard classical model Hamiltonian

$$\mathcal{H}=-\tfrac{1}{2}J\sum_{\langle ij\rangle}\mathbf{S}_i\cdot\mathbf{S}_j \tag{2}$$

was simulated where $\mathbf{S}_i=(S_x,S_y,S_z)$ is a unit three vector and J is the nearest-neighbor exchange constant. $J<0$ corresponds to an antiferromagnetic interaction.

The simulations were carried out using the standard

Metropolis spin-flipping algorithm with three system sizes $L\times L\times L=2\times 2\times 2$, $4\times 4\times 4$, and $6\times 6\times 6$ unit cells. It is important to keep in mind that there are 16 spins per cubic unit cell which corresponds to lattice sizes of $128(L=2)$, $1024(L=4)$, and $3456(L=6)$ spins, respectively. Thus, the largest lattice considered is roughly comparable to a $15\times 15\times 15$ Bravais lattice. Simulation lengths varying from 5000 to 200 000 Monte Carlo Steps (MCS) per spin were carried out over a wide range of temperatures $0.05\geq T/J\geq 20.0$ we use units in which $k_\beta=1$. For each simulation between 1000 and 10 000, initial MCS were discarded in order to reach equilibrium. The longest simulations were done at low temperatures. The random-spin moves $\Delta\mathbf{S}$ in the Metropolis algorithm were attenuated by a factor δ that was adjusted in such a way that roughly 50% of the attempted spin moves were accepted. This increases the efficiency at low temperatures. When a spin move was rejected, the spin was then randomly pivoted around its local exchange field.[30] Such pivoting has no effect on the internal energy but does increase the rate at which phase space is sampled.

All thermodynamic functions were calculated using histogram or reweighting methods.[31] This method allows efficient storage and usage of the MC data and most notably the method allows one to calculate all thermodynamic properties as continuous functions of temperature.

The central idea behind the histogram method is to build up information on the energy probability distribution $P_\beta(E)$, where $\beta=1/T$ is the inverse temperature. To be more specific, one calculates a histogram $H_\beta(E)$ which is the number of spin configurations generated between E and $E+\Delta E$. $P_\beta(E)$ is now defined as

$$P_\beta(E_\nu)=\frac{H_\beta(E_\nu)}{\mathcal{Z}_\beta}\ , \tag{3}$$

$$\mathcal{Z}_\beta=\sum_\nu H_\beta(E_\nu)\ . \tag{4}$$

Through a simple transformation,[31] one can, in principle, also calculate the probability distribution at any temperature β':

$$P_{\beta'}(E_\nu)=\frac{P_\beta(E_\nu)\exp[(\beta-\beta')E_\nu]}{\sum_\mu P_\beta(E_\mu)\exp[(\beta-\beta')E_\mu]}\ . \tag{5}$$

In practice, $P_\beta(E)$ only provides information on the distributions at nearby temperatures since counting statistics in the wings of the distribution $H_\beta(E)$ far from $\langle E\rangle_\beta$ (the average energy) will be poor.

In order to alleviate this problem, Ferrenberg and Swendsen have proposed the "multihistogram method," which is an optimized method of combining histogram data for different temperatures and has been implemented in our calculations. In order to follow with temperature quantities like the sublattice magnetization m_s, one must store two-dimensional histograms in the form $H_\beta(E,m_s)$. Storing two-dimensional histograms is quite costly and can be circumvented if one is only interested in calculating the thermodynamic quantities at one value of the applied field (i.e., $H=0$). The idea is to store a one-dimensional histogram $H_\beta(E)$ along with $\langle m_s(E)\rangle_\beta$, $\langle[m_s(E)]^2\rangle_\beta$, which allows calculation of $\langle m_s\rangle,\chi_s$ as continuous functions of temperature.[32]

Each histogram contained 5000 bins spread over an energy range from $E/|J|=-1$ to $+0.5$ for high temperatures and from $E/|J|=-1$ to -0.9 for the very low temperatures. This corresponds to bin sizes of $\Delta E/|J|=3\times 10^{-4}$ and 2×10^{-5}, respectively. As a check, some histograms with 20 000 bins were calculated for $L=4$ and $L=6$ and gave virtually identical results.

In order for the multiple histogram method to function properly, the histograms $H_\beta(E)$ for neighboring temperatures must have some overlap. At high temperatures $H_\beta(E)$ tends to be rather broad and histograms at widely spaced temperature intervals are sufficient. At low temperatures, simulations must be done at much smaller temperature intervals. As well, $H_\beta(E)$ narrows like $V^{-1/2}$ with system volume which implies that calculating thermodynamic quantities over a wide temperature range for large lattices is quite time consuming. The simulation time will increase as $V^{3/2}$ or $L^{9/2}$ in this case. For $L=6$ it was necessary to combine 193 histograms. However, once the histogram data is generated, all primary thermodynamic properties will be available at arbitrarily fine-temperature intervals. This virtually eliminates the possibility of missing any very narrow features (in temperature) that could be associated with a phase transition. The thermodynamic functions were calculated at temperature intervals of $\Delta T/|J|=0.001$ and 0.01, respectively, in the low- and high-temperature regimes.

Assuming standard counting statistics, errors can be estimated as

$$\sigma_{H(E)}=[\tau H(E)]^{1/2}\ , \tag{6}$$

where τ is the auto correlation time. These errors can be carried through in the calculation of all thermodynamic quantities. For our problem, the heat capacity seemed to be the most sensitive to statistical error.

III. ELEMENTARY THERMODYNAMIC PROPERTIES

The internal energy and heat capacity are shown in Fig. 2. If any phase transition occurs, it is expected to be at some temperature below the mean-field T_c indicated by the arrow. A transition to LRO should be accompanied by noticeable finite-size effects, particularly in the heat capacity, which result from a correlation length larger than the simulation size. Except for minimal noise in the heat-capacity data, there are no anomalies or finite-size effects. For the heat capacity which was the most sensitive to statistical noise, a few sample error bars are shown, where τ in (6) was estimated at $\tau\approx 5$ MCS, based on plots of $E(t)$ vs $E(t+\tau)$. At low temperature, the internal energy is seen to approach an expected ground-state energy of $-1.0|J|$. An asymptotic fit to the energy at low temperature gives $E(T=0)=-1.0|J|$ to within 0.01% with a slope

$$dE/dT|_0=C_H(T=0)\approx 0.71(1)\ .$$

This result is hard to reconcile with spin-wave theory (and the equipartition theorem) for an ordered magnet, which predicts that the zero-temperature heat capacity should be $C=1$ ($\frac{1}{2}$ for each transverse degree freedom). This provides further evidence that there is no LRO at low temperature.

In light of the fact that the order parameter for this model is not known, we have chosen to calculate the mean sublattice magnetization which is a measure of the $\mathbf{q}=0$ Fourier modes:

$$m_s^2=\frac{4}{N^2}\left\langle \sum_{a=1}^{4} m_a^2 \right\rangle . \tag{7}$$

where

$$\mathbf{m}_a=\sum_i \mathbf{S}_i^a . \tag{8}$$

Here i labels a unit cell and a labels a sublattice within the unit cell. The sublattice magnetization and its associated staggered susceptibility are shown in Fig. 3. The size dependence of m_s is typical for the behavior of rms (root mean square) magnetization variables in the paramagnetic regime of finite systems. The log-log plot of the susceptibility indicates a roughly T^{-1} behavior over about two and a half decades in temperature. Since χ_s is defined by

$$\chi_s=N\frac{J}{T}(\langle m_s^2\rangle-\langle m_s\rangle^2) , \tag{9}$$

we see that the average fluctuations in m_s remain roughly constant at all temperatures.

Another quantity that is sensitive to the occurrence of phase transitions is the fourth energy cumulant suggested by Binder[33]

$$V_L=1-\frac{\langle E^4\rangle}{3\langle E^2\rangle^2} . \tag{10}$$

This quantity is a measure of the deviation of the energy probability distribution from a Gaussian form. Away from a phase transition or fixed point, $V_L\approx\frac{2}{3}$, and a minimum in V_L occurs at fixed points. The minimum of V_L is usually rather sensitive to finite-sized effects. In Fig. 4 one can see that $V_L=\frac{2}{3}$ at low temperatures and the only finite-size effects seem to be associated with the fixed point at $T=\infty$.

So far the data indicate no evidence for critical behav-

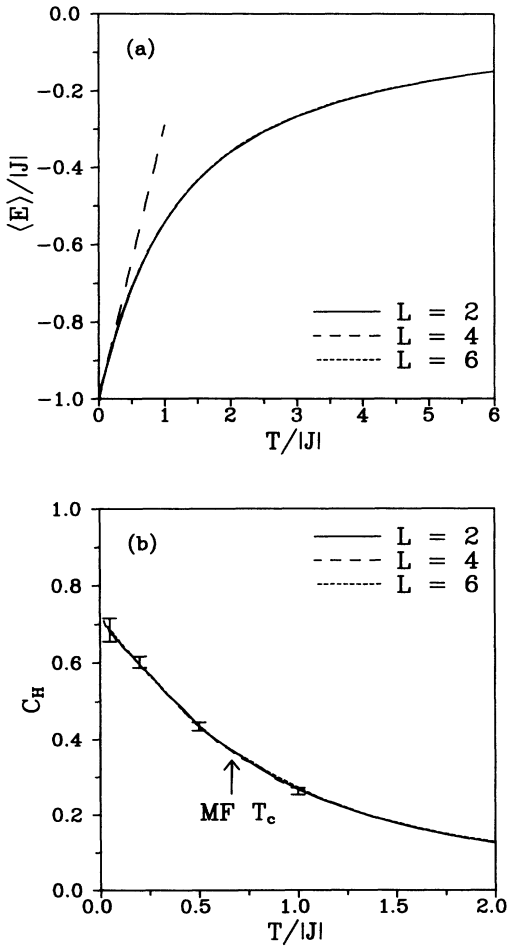

FIG. 2. (a) Internal energy and (b) the heat capacity per spin, for the pyrochlore NN antiferromagnet. The arrow indicates the mean field T_c.

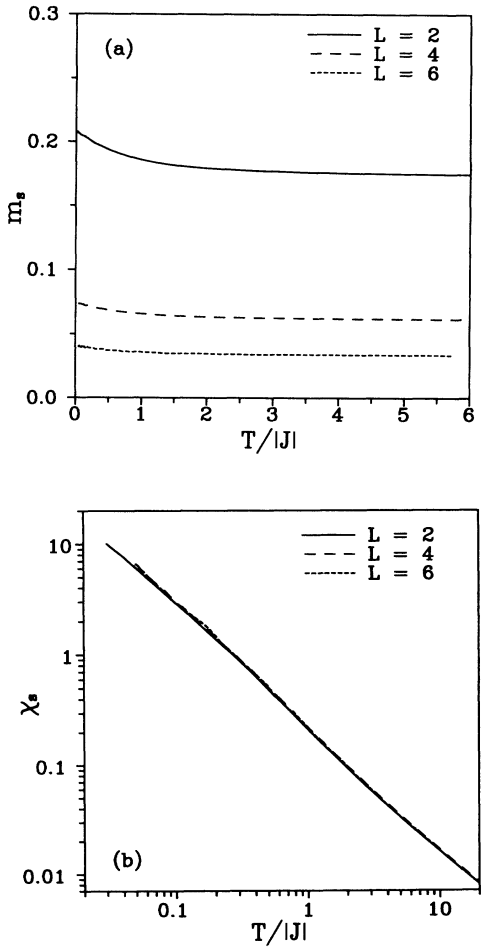

FIG. 3. (a) The $\mathbf{q}=\mathbf{0}$ sublattice magnetization and (b) its associated susceptibility per spin, for the pyrochlore NN antiferromagnet.

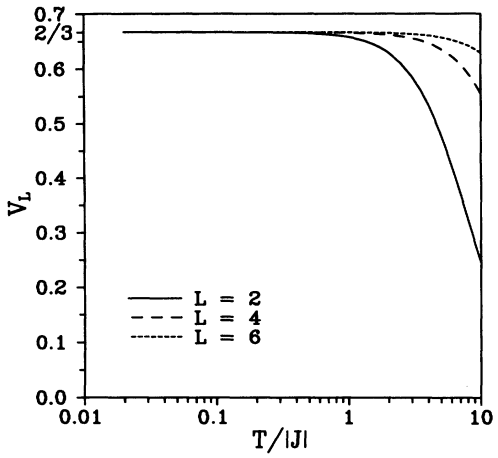

FIG. 4. The fourth energy cumulant (see text) indicating finite-size effects only at high temperature.

ior in the bulk properties. The mean-field-theory results[9] predict that further-neighbor interactions will stabilize LRO. Figure 5 shows the critical temperatures for a model with a next-nearest-neighbor interaction J_{NNN} as a function of $J_{\mathrm{NNN}}/|J|$. In this model, which is discussed in more detail in Refs. 9 and 34, the $\mathbf{q}=0$ modes are stabilized. These data were calculated by MC simulations on a $4\times4\times4$ lattice, again using the histogram method which provides rather accurate estimates for critical temperatures. The T_c's were define by the maxima in C_H and χ_s. It seems clear that $T_c\rightarrow0$ as $J_{\mathrm{NNN}}\rightarrow0$. The solid lines, which are fits to a power law, are merely intended as guides to the reader's eye.

IV. SCATTERING FUNCTION

One remaining possibility is that a very weak transition to some sort of incommensurate LRO has occurred. Without a *priori* knowledge of the wave vector for the incommensurate LRO, this may be difficult to detect. An efficient way to check for LRO of a general sort is to calculate the neutron-scattering function from the low-temperature spin configurations. Any LRO would show up as Bragg peaks which will grow in intensity like N^2 and narrow like L^{-1}. Thus sharp peaks in the scattering function that show dramatic lattice size dependence should be present if LRO has occurred. Even incommensurate structures that do not fit within the periodic boundary conditions should show some size dependence. In order to inspect the data in a one-dimensional form, we will calculate the radial part of the scattering which corresponds to the data observed in a powder diffraction experiment.

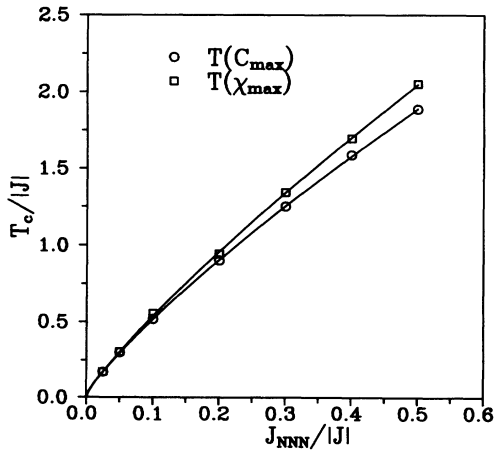

FIG. 5. Dependence of T_c on J_{NNN} for a model with a NNN interaction that exhibits LRO. Apparently T_c goes to zero as J_{NNN} approaches zero. The solid lines, which are fits with a power law, are merely intended as guides to the reader's eye.

After performing an angular average in Q space,[35] the magnetic neutron cross section for a system with one type of magnetic atom is

$$\frac{d\sigma}{d\Omega}(Q)=\tfrac{2}{3}[\tfrac{1}{2}f(Q)\gamma r_0]^2\frac{1}{Q}\times\sum_{\langle ij\rangle}\langle\mathbf{S}_i\cdot\mathbf{S}_j\rangle\frac{\sin(QR_{ij})}{R_{ij}}\ , \tag{11}$$

where $f(Q)$ is the magnetic form factor, $\frac{1}{2}\gamma r_0=0.27\times10^{-12}$ cm/μ_B is the neutron-scattering length per Bohr magneton, Q is the magnitude of the scattering vector, and the factor of $\frac{2}{3}$ takes account of the fact that neutrons are only scattered by the portion of the spin vectors that are perpendicular to the scattering vector Q. This is essentially just a version of the standard Debye formula adapted for magnetic spin scatterers. If the spins are correlated over large distances, the double summation in (11) will be proportional to N^2, whereas for short-range order it will be proportional to N.

In order to compare the results for different lattice sizes, we will plot the scattering per spin, $(d\sigma/d\Omega)/N$. As well, the magnetic form factor $f(Q)$, which merely attenuates the signal at high Q, has been divided out. A unit-cell edge of $a_{\mathrm{cell}}=10$ Å, which is typical for pyrochlores, has been assumed in order to give the scattering vector appropriate units. The result is shown in Fig. 6(a) for two temperatures. In the Q range considered, two broad peaks are apparent with no size effects observed for $T/|J|=1$. However, at the very low temperature $T/|J|=0.05$, the $L=2$ data deviates slightly from data for larger lattices but the $L=4$ and 6 profiles are virtually identical. This implies that there are some weak correlations beyond two unit-cell lengths but not beyond four cell lengths. In order to appreciate the diffuse nature of the scattering in Fig. 6(a), the scattering function for the model with a NNN interaction is shown in Fig. 6(b). Here the development of Bragg-like peaks, which grow with lattice size and also become sharper for the larger lattices, is obvious. The diffuse scattering in Fig. 6(a) is due to small correlated droplets whose spatial extent is roughly two unit cells. This result essentially eliminates the possibility of any incommensurate order with a very weak phase transition.

The scattering in Fig. 6(a) can be compared (after scaling with an appropriate form factor) directly with experimental neutron-diffraction results for FeF_3,[36] $Y_2Mn_2O_7$,[21] and $Tb_2Mo_2O_7$.[24,25] FeF_3 does exhibit LRO below 16 K; however, over a wide temperature range from T_c to $10T_c$,

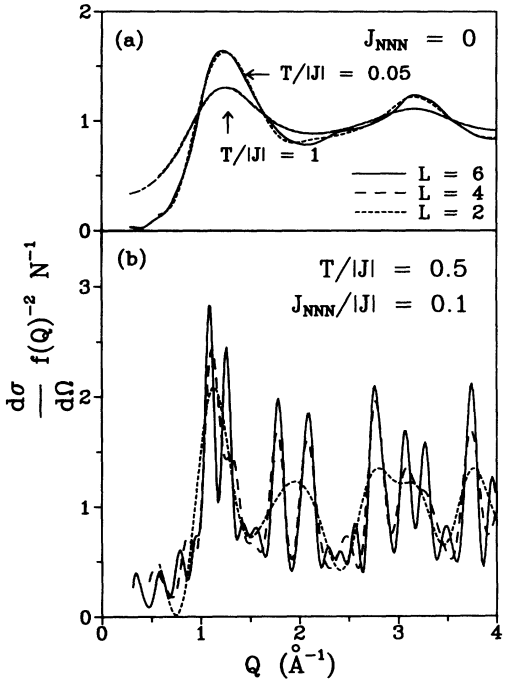

FIG. 6. Powder neutron-scattering profiles calculated from spin configurations generated by Monte Carlo simulations at low temperature. (a) Diffuse scattering arising from short-range correlations and (b) Bragg-like scattering from the model with a NNN interaction for comparison purposes.

diffuse magnetic scattering is observable. It is worth pointing out that the pseudo-Bragg scattering calculated from (11) is not comparable to experiment because the derivation of (11) assumes isotropy in spin space which is broken in a long-range-ordered phase. The positions of Bragg-like peaks will be correct but relative intensities will not be.

V. SPIN NEMATIC ORDER

In a collinear spin nematic, the spins are all oriented along an arbitrarily selected single axis in spin space. The actual polarity of the spins is, however, not long-range ordered. Thus, nematic order is not characterized by an ordering wave vector but by a tensor

$$Q^{\alpha\beta}=\frac{1}{N}\sum_i [\langle S_i^\alpha S_i^\beta\rangle - \tfrac{1}{3}\delta^{\alpha\beta}] .$$

Diagonalizing $Q^{\alpha\beta}$ determines a suitable coordinate system in spin space and the eigenvalues (λ) characterize the type of long-range nematic order. At low temperature, where $\langle S_i\rangle \approx 1$, three simple cases can be distinguished: (1) $\lambda=(0,0,0)$, no long-range nematic order, (2) $\lambda=(-\frac{1}{3},-\frac{1}{3},\frac{2}{3})$, collinear nematic order, and (3) $\lambda=(\frac{1}{6},\frac{1}{6},-\frac{1}{3})$, coplanar order, where the λ's are eigenvalues of $Q^{\alpha\beta}$. These eigenvalues have been calculated at two temperatures, $T/|J|=0.2$ and 0.05 for lattice sizes $L=2$, 4, and 6, and simulation lengths of 5000 MCS, which is longer than the relaxation time as determined in the next section. The results for $\lambda^{\rm rms}=(\lambda_1^2+\lambda_2^2+\lambda_3^2)^{1/2}$ are shown in Table I. Clearly all eigenvalues are extremely small ($\ll\frac{1}{6}$) indicating no long-range nematic order at these temperatures. A more detailed investigation of nematic order will be carried out in a future publication.

TABLE I. Root-mean-square eigenvalue $\lambda^{\rm rms}$ of the spin nematic ordering tensor $Q^{\alpha\beta}$. Nonzero eigenvalues indicate long-range nematic order.

	$T/\|J\|=0.2$	$T/\|J\|=0.05$
$L=2$	6×10^{-3}	1×10^{-2}
$L=4$	1×10^{-4}	6×10^{-3}
$L=6$	3×10^{-4}	2×10^{-3}

VI. DYNAMICS

In the absence of conventional LRO, it seems natural to investigate the behavior of some spin-glass order parameters. The Edwards-Anderson (EA) order parameter[1,37] and the autocorrelation function are defined by

$$q_{\rm EA}(t)=\frac{1}{N}\sum_{\rm r}\left[\frac{1}{t}\sum_{t'=0}^{t} S_{\rm r}(t')\right]^2=\frac{1}{N}\sum_{\rm r}\langle S_{\rm r}\rangle^2(t) , \quad (12)$$

$$\Psi(t)=\frac{1}{N}\sum_{\rm r}\langle \mathbf{S}_{\rm r}(0)\cdot\mathbf{S}_{\rm r}(t)\rangle , \quad (13)$$

respectively. As $t\to\infty$, one expects that $q_{\rm EA}(t)=\Psi(t)$.

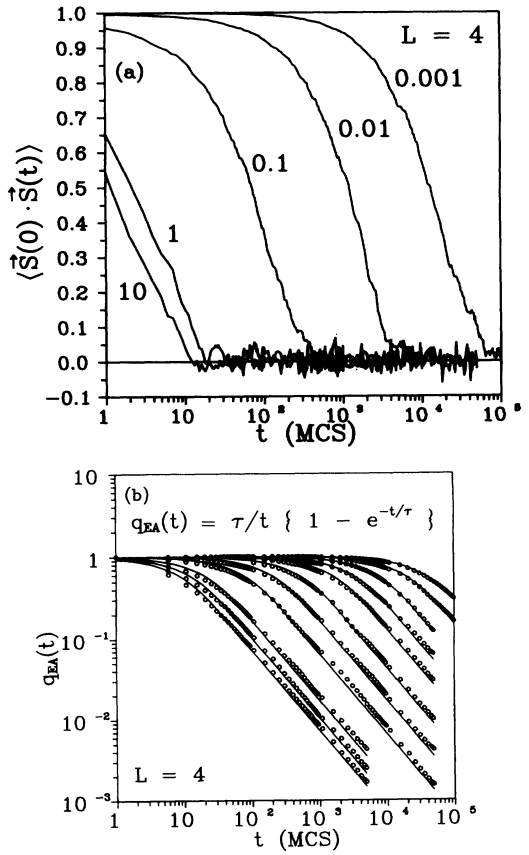

FIG. 7. Time dependence (in Monte Carlo Steps per spin) of (a) the autocorrelation function and (b) the EA order parameter (see text), for various temperatures from $T=2|J|$ down to $T=0.001|J|$.

Figure 7 shows the time dependence of these quantities for a wide range of temperatures. The solid lines in Fig. 7(b) represent fits to the empirical relationship

$$q_{\mathrm{EA}}(t)=\frac{\tau}{t}\left[1-\exp\left[-\frac{t}{\tau}\right]\right], \tag{14}$$

where the parameter τ can be interpreted as a relaxation time. One can see that, when $T<|J|$, the relaxation time grows rapidly. Figure 8 shows the temperature dependence of τ for the two lattice sizes investigated. The calculation was also repeated with no spin pivoting on rejected moves as this is expected to have an effect on the dynamics. The relaxation times were indeed about five times longer when spin pivoting was turned off. However, the qualitative temperature dependence was the same. At low temperature, τ seems to roughly follow a power law

$$\tau \propto T^{-1.25}, \tag{15}$$

which is consistent with spin freezing only at zero temperature.

These dynamical results should not be interpreted too literally since vector spins do not obey the stochastic dynamics of the MC method. However, Binder[38] and Fernandez[30] have successfully investigated vector spin dynamics from MC simulations, giving arguments that the qualitative dynamical behavior should be the same. In reality, the system will display a mixture of stochastic dynamics (induced by lattice vibrations) and spin motion due to the equations of motion. For classical spins, the equations of motion are

$$\frac{d\mathbf{S}_i}{dt}=\mathbf{S}_i\times\mathbf{H}_i^{\mathrm{eff}}, \tag{16}$$

where $\mathbf{H}_i^{\mathrm{eff}}$ is the local effective field at site i. As it turns out, the spin pivoting employed in the MC algorithm mimics (16) to some extent and, as we have seen, does not effect the qualitative behavior of the dynamics.

The fact that $q_{\mathrm{EA}}(t)\rightarrow 0$ as $t\rightarrow\infty$ at all finite temperatures is consistent with and reinforces the previous results showing the lack of any phase transition. The absence of size effects in τ indicates that there is no critical slowing down at finite temperature.

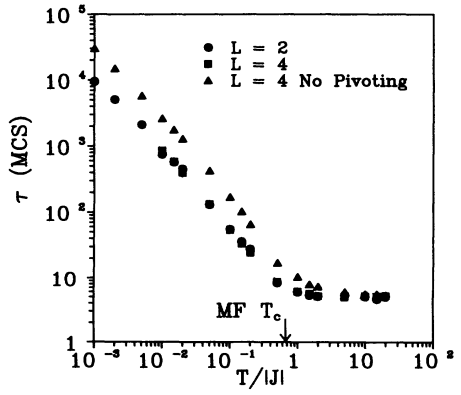

FIG. 8. Temperature dependence of the relaxation time τ obtained from an empirical fit (see text) of the EA order parameter.

VII. CONCLUSIONS

There are a number of models with no LRO at finite temperature that do order at $T=0$. All classical one-dimensional systems and the two-dimensional (2D) Heisenberg model are examples. In these systems, the density of states above the ground-state manifold is so high that entropy effects will destroy LRO at any nonzero temperature. There are also some interesting systems such as the fcc Ising antiferromagnet with infinite ground-state degeneracy [$S(0)\propto N^{1/3}$, which translates to zero entropy per spin] that order at finite temperature due to entropic selection.[5] This is opposite to the situation for one-dimensional systems. Finally, there are models that remain paramagnetic at all temperatures. Examples include the 2D antiferromagnetic triangular lattice with Ising spins[39] and Kagomé lattices with Ising or vector spins.[8,29] All of the evidence indicates that the pyrochlore NN antiferromagnet belongs to this last group.

The following observations from our simulations preclude the possibility of LRO in the temperature range considered: (1) absence of any maxima or finite-size effects in the heat capacity, (2) zero-temperature heat capacity $C_H(T=0)\neq 1$, (3) no minima in V_L except at $T=\infty$, (4) T_c for NNN model approaches zero as J_{NNN} goes to zero, (5) the scattering function shows no sharp peaks or size effects that would be associated with LRO, (6) the spin-glass order parameters approach zero at all finite temperatures, and (7) there are no finite-size effects in the dynamics. The lack of finite-size effects in all calculated properties is important because this can only be understood if one assumes that the spin-spin correlations do not extend beyond a distance on the order of two unit-cell lengths. The MC results show clearly that, if any thermal selection does occur, it is insufficient to stabilize LRO in the temperature range considered. The possibility of LRO at temperatures below $T=|J|/20$ still exists, however, MC is not efficient at such low temperatures. When one considers the finite-temperature results together with the finite number of continuous degrees of freedom in the ground state, an extremely low-temperature conventional LRO phase seems unlikely.

In light of these results, it is useful compare the pyrochlore lattice of corner-sharing tetrahedra with the fcc lattice of edge-sharing tetrahedra. To begin with, the corner-sharing lattice is more sparsely connected than the edge-sharing counterpart, as the names imply. This in itself will inhibit LRO. A more precise comparison can made by considering ground-state degeneracies. The ground state for the fcc Ising antiferromagnet is $N^{1/3}$-fold degenerate, which is a much smaller degeneracy than the N-dimensional degeneracy in the pyrochlore case. The two-dimensional continuous degeneracy of type-I fcc vector antiferromagnets is also small in comparison. The degeneracies for the fcc models are broken by thermal fluctuations. In the Ising case, LRO is stabilized and, in the vector spin case, a collinear structure is selected. It is

quite possible that thermal fluctuations will select a subset of the large ground-state manifold in pyrochlores, but that this subset is not restrictive enough to produce a long-range-ordered phase.

It would be interesting to investigate the system using a molecular-dynamics approach or quantum MC techniques. A proper dynamical treatment may give some understanding of the spin-glass-like behavior experimentally in pyrochlore antiferromagnets. Also, the effects of small levels of disorder should be investigated, i.e., will 5% chemical disorder induce spin freezing at nonzero temperature?

ACKNOWLEDGMENTS

This work has benefited considerably from informative discussions with C. L. Henley. I would also like to thank B. D. Gaulin for a critical reading of this manuscript and C. Kallin, J. R. Dahn, and J. E. Greedan for providing computer facilities used in this work. Private communications with A. M. Ferrenberg concerning implementation of the histogram method are also greatly appreciated.

*Present address: Department of Physics, Simon Fraser University, Burnaby, British Columbia, Canada V5A 1S6.

[1]K. Binder and A. P. Young, Rev. Mod. Phys. **58**, 801 (1986).
[2]J. M. Coey, Can. J. Phys. **65**, 1210 (1987).
[3]H. Kawamura, J. Phys. Soc. Jpn. **58**, 584 (1989); T. E. Mason, B. D. Gaulin, and M. F. Collins, Phys. Rev. B **39**, 586 (1989); H. Kadowaki, K. Ubukoski, K. Hirakawa, J. L. Martinez, and G. Shirane, J. Phys. Soc. Jpn. **58**, 584 (1989).
[4]A. N. Berker, G. S. Crest, C. M. Soukoulis, D. Blankschtein, and M. Ma, J. Appl. Phys. **55**, 15 (1984); D. Blankschtein, M. Ma, A. N. Berker, G. S. Grest, and C. M. Soukoulis, Phys. Rev. B **29**, 5250 (1984); R. R. Netz and A. N. Berker, Phys. Rev. Lett. **66**, 377 (1991).
[5]A. Dannielian, Phys. Rev. **133**, A1344 (1964).
[6]P. W. Anderson, Phys. Rev. **102**, 1008 (1956).
[7]J. Villian, Z. Phys. B **33**, 31 (1978).
[8]R. Liebmann, *Statistical Mechanics of Periodic Frustrated Ising Systems* (Springer, Berlin, 1986), p. 117.
[9]J. N. Reimers, A. J. Berlinsky, and A.-C. Shi, Phys. Rev. B **43**, 865 (1991).
[10]A. B. Harris, A. J. Berlinsky, and C. Bruder, J. Appl. Phys. **69**, 5200 (1991).
[11]J. S. Smart, *Effective Field Theories of Magnetism* (Saunders, Philadelphia, 1966).
[12]C. L. Henley, J. Appl. Phys. **61**, 3962 (1987).
[13]J. Villian, R. Bidaux, J. P. Carton, and R. J. Conte, J. Phys. (Paris) **41**, 1263 (1980).
[14]D. Babel, Z. Anorg. Allg. Chem. **387**, 161 (1972).
[15]M. Alba, J. Hammann, C. Jacoboni, and C. Pappa, Phys. Lett. **89A**, 423 (1982).
[16]L. Bevaart, P. M. H. L. Tegelaar, A. J. van Duyneveldt, and M. Steiner, Phys. Rev. B **26**, 6150 (1982).
[17]C. Pappa, J. Hammann, and C. Jacoboni, J. Magn. Magn. Mater. **31-34**, 1391 (1983).
[18]C. Jacoboni, Ph.D. thesis, Université de Paris VI, 1975.
[19]W. Kurtz, and S. Roth, Physica B **86-88**, 715 (1977); W. Kurtz, R. Geller, H. Dachs, and P. Convert, Solid State Commun. **18**, 1479 (1976).
[20]M. A. Subramanian, C. C. Torardi, D. C. Johnson, J. Pannetier, and A. W. Sleight, J. Solid State Chem. **72**, 24 (1988).
[21]J. N. Reimers, J. E. Greedan, R. K. Kremer, E. Gmelin, and M. A. Subramanian, Phys. Rev. B **43**, 3387 (1991).
[22]J. E. Greedan, M. Sato, X. Yan, and F. S. Razavi, Solid State Commun. **59**, 895 (1986).
[23]J. N. Reimers and J. E. Greedan, J. Solid State Chem. **72**, 390 (1988).
[24]J. N. Reimers, J. E. Greedan, S. L. Penny, and C. V. Stager, J. Appl. Phys. **67**, 5967 (1990); J. E. Greedan, J. N. Reimers, C. V. Stager, and S. L. Penny, Phys. Rev. B **43**, 5682 (1991).
[25]J. N. Reimers, B. D. Gaulin, Z. Tun, T. E. Mason, and J. E. Greedan (unpublished).
[26]C. Broholm, G. Aeppli, G. P. Espinsoa, and A. S. Cooper, J. Appl. Phys. **67**, 5799 (1990).
[27]A. P. Ramirez, G. P. Espinosa, and A. S. Cooper, Phys. Rev. Lett. **64**, 2070 (1990).
[28]C. Broholm, G. Aeppli, G. P. Espinosa, and A. S. Cooper, Phys. Rev. Lett. **65**, 3173 (1990); **66**, 522(E) (1991).
[29]V. Elser, Phys. Rev. Lett. **62**, 2405 (1989).
[30]J. F. Fernandez and T. S. J. Streit, Phys. Rev. B **25**, 6910 (1982).
[31]A. M. Ferrenberg and R. H. Swendsen, Phys. Rev. Lett. **61**, 2635 (1988); **63**, 1195 (1988); Comput. Phys. **Sep/Oct.**, 101 (1989); E. P. Münger and M. A. Novotny, Phys. Rev. B **43**, 5773 (1991).
[32]A. M. Ferrenberg (private communication).
[33]K. Binder, Z. Phys. B **43**, 119 (1981).
[34]J. N. Reimers, J. E. Greedan, and M. E. Björgvinnsen, following paper, Phys. Rev. B **45**, 7295 (1992).
[35]E. F. Bertaut and P. Burlet, Solid State Commun. **5**, 279 (1967).
[36]J. N. Reimers, J. Greedan, C. V. Stager, and M. Björgvinnsen, Phys. Rev. B **43**, 5692 (1991).
[37]S. F. Edwards and P. W. Anderson, J. Phys. F **5**, 965 (1985).
[38]K. Binder, Z. Phys. B **26**, 339 (1979).
[39]G. H. Wannier, Phys. Rev. **79**, 357 (1950).